



ELSEVIER

MICROPOROUS AND  
MESOPOROUS MATERIALS

Microporous and Mesoporous Materials 37 (2000) 41–48

[www.elsevier.nl/locate/micromeso](http://www.elsevier.nl/locate/micromeso)

# One-step synthesis of high capacity mesoporous $Hg^{2+}$ adsorbents by non-ionic surfactant assembly

Jennifer Brown, Roger Richer, Louis Mercier \*

*Department of Chemistry and Biochemistry, Laurentian University, Sudbury, Ontario P3E 2C6, Canada*

Received 19 July 1999; accepted for publication 8 October 1999

## Abstract

We report the first example of a one-step preparation route towards high capacity mesostructured heavy metal ion adsorbents with uniform mesopore diameters. The synthesis approach involved the co-condensation of TEOS and (3-mercaptopropyltrimethoxysilane) in the presence of structure-directing non-ionic Triton-X100 surfactant micelles. One such material, denoted MP(2)-MSU-2, had a uniform pore diameter distribution centered at 28 Å and a  $Hg^{2+}$  loading capacity of 2.3 mmol/g, making its effectiveness for mercury ion trapping comparable to that of the highest capacity materials previously reported. The total access of the  $Hg^{2+}$  ions to every complexation site in the adsorbents was also demonstrated. Treating the  $Hg$ -loaded adsorbents with concentrated HCl was found to remove the bound mercury ions and regenerate the material for further adsorption. © 2000 Elsevier Science B.V. All rights reserved.

**Keywords:** Adsorbent; Mercury; Mesoporous; Mesostructure; One-step synthesis

## 1. Introduction

The presence of mercury in the environment is of serious social and environmental concern, prompting the establishment of increasingly stringent government regulations demanding that levels of this contaminant be lowered. In order to address this issue, an encouraging branch of research has evolved in recent years involving the synthesis of rationally designed materials capable of specifically removing mercury and other heavy metal ions from aqueous systems [1–10]. In particular, materials whose surfaces have been functionalized with mercury-binding thiol groups have shown extraordinary promise for the mitigation of mercury levels in the environment [1,2,5–10].

\* Corresponding author. Fax: +1-705-6754844.

E-mail address: lmercier@nickel.laurentian.ca (L. Mercier)

(Thiol-functionalized mesostructured silicas of the type MCM-41 and HMS have recently gained recognition as the most exceptional adsorbents for heavy metal ion trapping [5–10].) These materials were first prepared by the surface anchoring or grafting of 3-mercaptopropyltrialkoxysilane [MPTS,  $(RO)_3Si(CH_2)_3SH$ , where  $R = CH_3$  or  $CH_2CH_3$ ], a potent ligand for heavy metal ion binding, onto preformed mesostructured silica [5,6]. These materials, labeled MP-HMS [5] and FMMS [6], exhibited unprecedentedly high loading capacities for  $Hg^{2+}$  (1.5 and 2.5 mmol/g, respectively). Unlike most other chelating adsorbents, both these materials were able to bind  $Hg^{2+}$  ions to every thiol group in their structures, a phenomenon attributable to the uniform open-framework mesoporosity in the hybrid materials which allowed unhindered access of the metal ions to the binding sites [5]. Moreover, a noteworthy

property of thiol-functionalized mesostructures recently identified is their apparent binding specificity for mercury ions, to the exclusion of other metal ions ( $\text{Cd}^{2+}$ ,  $\text{Pb}^{2+}$  and  $\text{Zn}^{2+}$ ) normally expected to exhibit strong complexation affinity with thiol functions [10]. Thiol-functionalized mesostructures are thus uniquely promising materials for mercury contamination remediation, exhibiting both unsurpassed binding capacity as well as binding selectivity for mercury ions. However, commercialization of these materials may be impeded by the relatively high production cost of these materials. This is especially reflected in the high prices of the assembly surfactants, which are often consumed (calcined) during preparation of mesostructures [6], as well as that of the organosilane used to functionalize the materials. Exploration of alternate synthesis strategies for these adsorbents may thus afford the discovery of more cost-effective preparation techniques.

An attempt to simplify the preparation of such adsorbents was demonstrated by directly incorporating MPTS into an MCM-41-type mesostructure using a one-step synthesis approach [8]. The reduced synthesis time, the removal/recovery of the framework-forming surfactants by acid extraction, and the minimal waste of the MPTS reagent represent significant advantages over the previously cited mesostructure grafting methods, potentially translating into notable reductions in adsorbent production costs compared with those of MP-HMS and FMMS. When tested for  $\text{Hg}^{2+}$  adsorption, this material was found to have a binding capacity close to that of FMMS (2.1 mmol/g). Because of the constriction caused by the abundant mercaptopropyl groups within its pore channels, this material was microporous (pore diameter 14 Å), a property which is likely to preclude the total access of the metal ions to the binding sites, as well as restrict their diffusion into the pore network [5]. The bench-top (non-hydrothermal) synthesis of silica mesostructures by cationic alkyltrimethylammonium assembly typically produces materials with lower-end mesoporosity (25 to 30 Å in diameter) [11]. Thus, the incorporation of large amounts of organosilane groups into these structures usually constricts the pore chan-

nels into the micropore range (below 20 Å) [8,11,12].

On the other hand, the preparation of mesostructures using non-ionic surfactants (including Tergitol and Triton-X) as structure-directing agents was shown to produce materials (denoted MSU-1 and MSU-2, respectively) with considerably larger pore diameters (above 30 Å) [13]. Moreover, it was reported that, under neutral pH conditions, the pore sizes of non-ionic surfactant-assembled mesostructures systematically increased as a function of synthesis temperature (within the range 25 to 65°C), producing materials with pore diameters up to 80 Å [14]. Recently, the co-condensation of organosiloxane molecules and TEOS in the presence of structure-directing non-ionic surfactant micelles was shown to be a promising synthesis strategy for the one-step preparation of organically functionalized mesoporous materials [15]. In this work, this latter concept was utilized, in combination with synthesis temperature control, to produce two highly mercaptopropyl-functionalized mesoporous  $\text{Hg}^{2+}$  adsorbents by single-step processes.

## 2. Experimental

### 2.1. Adsorbent syntheses

The first adsorbent, denoted MP(1)-MSU-2, was prepared by adding tetraethoxysilane (TEOS) (0.0265 mol) and mercaptopropyltrimethoxysilane (MPTMS) (0.00054 mol) to 100 ml of Triton-X100 solution (0.027 mol/l). Thus, the mercaptopropylsilane group content in this synthesis mixture represents 2% of the total silane content (MPTMS + TEOS). The mixture was stirred in a thermostated water bath set at 45°C until a clear homogeneous solution was obtained. NaF (0.00054 mol) was then added and, after 24 h of stirring, the precipitated product was filtered, air dried and washed by Soxhlet extraction over ethanol for 24 h.

The second adsorbent, denoted MP(2)-MSU-2, was prepared following the same protocol as that of MP(1)-MSU-2, except that 0.0257 mol of TEOS and 0.00135 mol of MPTMS were used. The mer-

captopropylsilane content in this mixture was 5% of the total silane content.

## 2.2. Characterization

Powder X-ray diffraction (XRD) patterns of the adsorbents were recorded on a Rigaku rotaflex diffractometer using Cu K $\alpha$  radiation. Nitrogen adsorption isotherms were measured at 77 K on a Micromeritics ASAP 2010 sorptometer, with the samples outgassed for 16 h at 110°C and 10<sup>-6</sup> Torr prior to measurement. Proton-decoupled <sup>29</sup>Si MAS NMR spectra were recorded on a Bruker AMX 200 MHz spectrometer at 39.8 MHz, with a pulse delay of 300 s to ensure full relaxation of the nuclei prior to each scan. C and S analyses on the samples were also performed (Laurentian University Central Analytical Facility). The physicochemical characteristics thus obtained for these materials are shown in Table 1.

## 2.3. Hg<sup>2+</sup> adsorption

A 20 mg portion of adsorbent [MP(1)-MSU-2 or MP(2)-MSU-2] was slurried in a flask containing 90 ml water. A 10 ml aliquot of a mixed metal ion solution [containing nitrate salts of Hg<sup>2+</sup> (115 ppm), Pb<sup>2+</sup> (147 ppm), Cd<sup>2+</sup> (53 ppm), Zn<sup>2+</sup> (110 ppm), Ni<sup>2+</sup> (38 ppm) and Cu<sup>2+</sup> (45 ppm)] was titrated into the suspension. After stirring covered for 24 h, a portion of the suspension was collected from the flask and centrifuged. A 10 ml aliquot of the clear supernatant liquid was collected, then the powder and solution remaining in the centrifuge tube were returned to the initial flask. The metal ion contents of the aliquot were measured by cold vapor atomic absorption

spectroscopy (AAS) for Hg and flame AAS for the other metals. This titration, collection and analysis cycle was repeated until the Hg level in the collected aliquots rose significantly (indicating saturation of the adsorbent). Adsorption isotherms for each metal ion were generated by plotting the amount of metal ion adsorbed per gram of material as a function of the equilibrium metal concentration.

## 2.4. Adsorbent regeneration

(A sample of the Hg-loaded MP(2)-MSU-2 was stirred in 100 ml of concentrated (12.1 M) HCl for 24 h. The material was then filtered and the amount of Hg leached out of the adsorbent was measured by cold vapor AAS. The uptake of Hg<sup>2+</sup> ions by the regenerated material was then determined, using the technique described in Section 2.3.)

## 3. Results and discussion

### 3.1. Adsorbent characterization

The powder XRD patterns of the adsorbents were consistent with those previously reported for wormhole framework motifs, as expected in materials formed by neutral and non-ionic surfactant assembly techniques [13–15]. The XRD pattern of MP(1)-MSU-2 showed a  $d_{100}$  reflection at  $2\theta = 1.40^\circ$ , corresponding to a  $d$ -spacing of 63 Å (Table 1), and a broad, low intensity  $d_{200}$  reflection is also observed at higher angle ( $\sim 3^\circ$ ). In contrast, the XRD pattern of MP(2)-MSU-2 showed a  $d_{100}$  reflection at  $2\theta = 1.80^\circ$ , corresponding to a  $d$ -

Table 1  
Physicochemical properties of mercaptopropyl-functionalized mesostructures

Material designation	Synthesis temperature (°C)	% MPTS in mixture	% MPTS in material	Thiol content in material (mmol/g)	$d_{100}$ lattice spacing (Å)	BET surface area (m <sup>2</sup> /g)	Pore diameter (Å)
MP-MSU-2-2% [15]	35	2.0	3.0	0.47	50	1176	27
MP-MSU-2-5% [15]	35	5.0	7.7	0.87	40	763	n.d.
MP(1)-MSU-2	45	2.0	6	0.9	63	1140	42
MP(2)-MSU-2	45	5.0	17	2.3	49	739	28

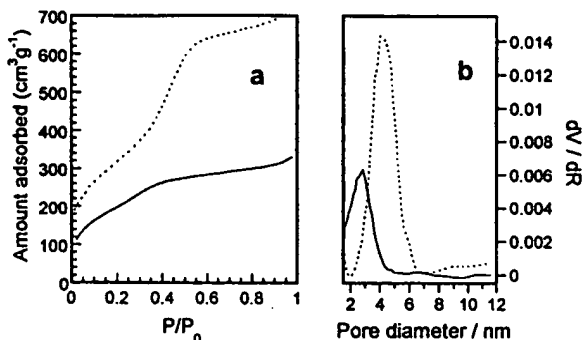


Fig. 1. (a)  $N_2$  adsorption isotherm and (b) corresponding pore size distribution for MP(1)-MSU-2 (dotted curves) and MP(2)-MSU-2 (solid curves).

spacing of 49 Å (Table 1), and no  $d_{200}$  reflection was observed. The reduced intensity of the  $d_{100}$  peak intensity and the lack of any observable  $d_{200}$  in MP(2)-MSU-2 is indicative of contrast matching resulting from the more abundant presence of thiol groups within the pore channels of the adsorbent [5,9]. The decreased lattice spacing for MP(2)-MSU-2 can be likewise attributed to the presence of larger amounts of organosilane in the synthesis mixture: consistent with recently reported findings, contraction of the framework lattice likely occurred because of a deeper penetration of the abundant organophilic mercaptopropylsilane molecule within the hydrophobic core of the surfactant micelles [15]. When compared with analogous materials prepared at lower synthesis temperatures (35°C) (Table 1) [15], both MP(1)-MSU-2 and MP(2)-MSU-2 are found to possess significantly larger lattice spacings. The higher mesostructure synthesis temperature thus increases the size of the micelles, resulting in the assembly of larger-framework materials [14].

$N_2$  adsorption/desorption measurements on both materials yielded hysteresis-free type IV isotherms with inflections observed between 0.35 and 0.50 for MP(1)-MSU-2, and between 0.15 and 0.35  $P/P_0$  for MP(2)-MSU-2 [Fig. 1(a)]. From these isotherms, the BET surface areas of the materials were determined [MP(1)-MSU-2: 1140  $\text{m}^2/\text{g}$ ; MP(2)-MSU-2: 739  $\text{m}^2/\text{g}$ ], the pore diameters calculated using the Horvath-Kawazoe method [16] [MP(1)-MSU-2: 42 Å; MP(2)-MSU-2: 28 Å] [Fig. 1(b)], and mesopore volumes

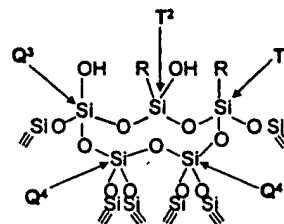


Fig. 2. Assignment of the  $^{29}\text{Si}$  NMR signals for the various Si sites present in the mesostructures ( $R = \text{CH}_2\text{CH}_2\text{CH}_2\text{SH}$ ).

estimated [MP(1)-MSU-2: 0.87  $\text{cm}^3/\text{g}$ ; MP(2)-MSU-2: 0.37  $\text{cm}^3/\text{g}$ ] (Table 1). The narrow pore size distributions found for both materials attest their uniform framework mesoporosity [15]. In contrast to the less functionalized MP(1)-MSU-2, the increased abundance of mercaptopropyl moieties incorporated within the pore channel walls of MP(2)-MSU-2 resulted in reduced surface area, pore diameter and pore volume. Despite the greater pore channel constriction in MP(2)-MSU-2, however, this material none the less retained significant mesoporosity.

The  $^{29}\text{Si}$  MAS NMR spectra of the materials showed four resonances at -60, -65, -101 and -110 ppm, which were assigned to the  $T^2$  [ $(\text{SiO})_2(\text{HO})\text{Si}(\text{CH}_2)_3\text{SH}$ ],  $T^3$  [ $(\text{SiO})_3\text{Si}(\text{CH}_2)_3\text{SH}$ ],  $Q^3$  [ $(\text{SiO})_3\text{SiOH}$ ] and  $Q^4$  [ $(\text{SiO})_4\text{Si}$ ] sites, respectively (Fig. 2) [8,11]. By comparing the relative integrations of these signals in both materials, their chemical compositions were determined as  $(\text{SiO}_2)_{0.63}(\text{SiO}_{2.5}\text{H})_{0.31}(\text{SiO}_{1.5}\text{C}_3\text{H}_6\text{SH})_{0.06}$  for MP(1)-MSU-2 and  $(\text{SiO}_2)_{0.49}(\text{SiO}_{2.5}\text{H})_{0.34}(\text{SiO}_{1.5}\text{C}_3\text{H}_6\text{SH})_{0.12}(\text{SiO}_2\text{HC}_3\text{H}_6\text{SH})_{0.05}$  for MP(2)-MSU-2. Based on these formulae (and corroborated by the results of the C and S analyses) the thiol group content in MP(1)-MSU-2 is 0.9 mmol/g, while that of MP(2)-MSU-2 is 2.3 mmol/g (Table 1). Remarkably, the stoichiometry of these materials is vastly different from that expected based on the composition of the solution mixture used to prepare the adsorbents. Despite the 2% and 5% mercaptopropylsilane molar percentages (with respect to TEOS) in the synthesis mixtures of MP(1)-MSU-2 and MP(2)-MSU-2, respectively, the materials obtained had functional group contents of 6% and 17%, respectively; about three times higher than what would be expected

based on the reagent stoichiometry. In a previous paper, such preferential assembly of mercaptopropyl groups at the interface of Triton-X micelles at 35°C was likewise observed, resulting in the formation of mesostructured compounds with increased loading of the functional groups (to about 150% of the solution composition) [15]. These observations suggest that the mesostructure assembly temperature is a synthesis factor that has important consequences not only for the structure of the material [14], but also for the composition of the resulting product. Recently, Prouzet and Pinnavaia demonstrated that the framework porosity of wormhole motifs assembled by non-ionic surfactant assembly can be systematically increased by raising the temperature of the synthesis [14]. Thus, increasing the synthesis temperature produces mesostructure with both larger pore diameters and increased organosilane group loading. This phenomenon was ascribed to the swelling of the hydrophobic core of the surfactant micelles at higher temperature caused by the breaking of hydrogen bonds between the ethylene oxide groups of the surfactant and the water molecules at increasing temperatures [14]. The results of this current work indicate that this same effect may also be responsible for the dissolution of a larger amount of the hydrophobic MPTMS molecules into the swelled micelle cores, producing a more highly functionalized mesostructure as crosslinking is catalyzed at the micelle interface upon NaF addition. This hypothesis is supported by the apparent correlation between the cross-sectional micelle hydrophobic core area and the mercaptopropyl group content in the materials prepared using either 2% or 5% MPTMS mixtures (Fig. 3). The organosilane dissolution in the 5% MPTMS mixture is markedly greater than that of the 2% mixture, possibly as a result of LeChâtelier's principle which dictates that the higher MPTMS concentration in the 5% mixture should drive more organosilane into the micelle than in the case of the 2% mixture.

It is noteworthy to mention that the synthesis yields for MP(1)-MSU-2 and MP(2)-MSU-2 are both about 30%, based on the total cross-linking of the TEOS and MPTMS used in the adsorbent preparations. Since, in the case of MP(2)-MSU-2,

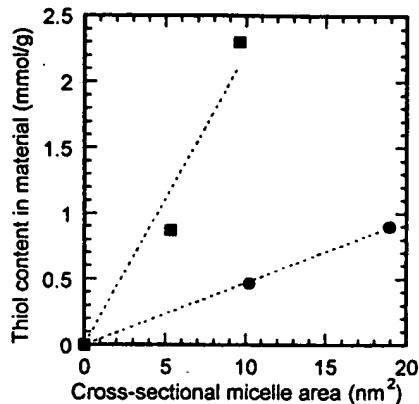


Fig. 3. Correlation between cross-sectional micelle areas and organosilane for thiol-functionalized MSU derivatives prepared using 2% organosilane mixtures (●) and 5% organosilane mixtures (■). The micelle areas ( $A$ ) were calculated from  $A = \pi(d/2)^2$ , where  $d$  is the assumed micelle diameter determined by subtracting the framework silica wall thickness (estimated as 1.5 nm for all mesostructures) from the  $d$ -spacings of each adsorbent (see Table 1).

the MPTMS loading is three times higher than that expected based on the reaction stoichiometry, the synthesis yield of the material can be no higher than 33%, since about two thirds of the TEOS used must remain unreacted in order to obtain a product with that stoichiometry. That the experimental yield of MP(2)-MSU-2 is below this threshold confirms that less than one third of the TEOS in the synthesis mixture forms the mesostructure. Further investigations are currently under way in our laboratory to elucidate in greater detail the effects of synthesis temperature, reaction mixture stoichiometry and organosilane leaving group on functionalized mesostructure formation.

In order to estimate the mercaptopropyl group density on the pore channel surface of MP(2)-MSU-2, the thiol moieties were considered as organic groups covering the surface of a non-functionalized mesoporous silica framework [6]. In the absence of any functionalization, the silica surface area and pore diameter were considered to be 900 m<sup>2</sup>/g and 35 Å, respectively (these values are typical of purely siliceous mesostructures prepared by non-ionic surfactant assembly having a  $d$ -spacing of 49 Å). Since an intact monolayer of organosilane molecules on a silica surface (100%

coverage) is expected to contain  $5 \times 10^{18}$  molecules/m<sup>2</sup> [6], one can calculate on the basis of the material stoichiometry an organic group surface coverage of 44% ( $2.2 \times 10^{18}$  mercaptopropyl groups/m<sup>2</sup>). For a homogeneous distribution of organic groups within the walls of the pore channels, this coverage corresponds to a separation of about 1 nm between adjacent thiol sites, indicating the presence of about 12 mercaptopropyl groups per pore channel cross-section. This functional group density is clearly superior to that of the post-synthetically grafted adsorbent MP-HMS (six groups per cross-section) [5], whose parent silica mesostructure (HMS) was structurally similar to the non-ionic surfactant assembled silica (surface area of 854 m<sup>2</sup>/g and pore diameter of 36 Å). The thiol group coverage in MP(2)-MSU-2, however, falls short of that in FMMS, in which a 76% coverage is reported [6].

### 3.2. Hg<sup>2+</sup> adsorption

The Hg<sup>2+</sup> adsorption isotherms of both adsorbents (Fig. 4) exhibited typical Langmuir behavior (type I). The maximum mercury ion adsorption capacities of these materials were 0.90 mmol/g (180 mg/g) for MP(1)-MSU-2 and 2.3 mmol/g (460 mg/g) for MP(2)-MSU-2 (Table 2). These values correspond exactly to the amount of thiol groups in both materials, indicating the total access of mercury ions to every complexing site in the uniform mesopore channels (Table 2) [5]. The very high mercaptopropyl group content in

MP(2)-MSU-2 thus resulted in an adsorption capacity which is markedly higher than that reported for MP-HMS (1.5 mmol/g) [5,9]. Despite its lower surface thiol group density, the adsorption capacity of the material is comparable to that of FMMS (2.5 mmol/g) [6], the highest capacity Hg<sup>2+</sup> mesostructure-based adsorbent reported to date. Both MP(1)-MSU-2 and MP(2)-MSU-2 also proved to have very strong affinity for mercury ions in solution, virtually eliminating the metal from the treated solutions. For instance, when only 20 mg of MP(2)-MSU-2 was added to 100 ml solutions containing up to 30 ppm Hg<sup>2+</sup>, the residual concentrations of mercury ions in the treated solutions were very close to or below the detection limits of the analysis technique (0.01 ppm).

Table 2 summarizes the Hg<sup>2+</sup> adsorption capacities and physicochemical features of all the thiol-functionalized mesostructures reported to date. A survey of the data shows that only adsorbents with mesopore-range channel diameters (>2.0 nm) allow total access of the mercury ions to the thiol binding sites (Hg/S molar ratio ≈ 1) [9]. With the exception of FMMS, one-step synthesis strategies are shown to generally produce functionalized mesostructures with greater thiol group contents (and hence greater Hg<sup>2+</sup> adsorption capacities) compared to post-synthesis grafting methods (Table 2). Thus, Stein and coworkers have recently reported the one-step synthesis of a very highly thiol-functionalized MCM-41-type framework [8], using an electrostatic surfactant assembly strategy. The abundant thiol groups lining the inherently small diameters of such mesostructures, however, resulted in the constriction of their pore channels into the micropore size domain (1.4 nm diameter) [8], thereby resulting in less-than-complete complexation with the material's thiol groups (Hg/S molar ratio = 0.45) (Table 2). On the other hand, the ambient temperature non-ionic surfactant assembly protocol presented in this work succeeded in producing a highly thiol-functionalized mesostructure [MP(2)-MSU-2] while maintaining pore channel mesoporosity. Although the thiol group content in MP(2)-MSU-2 is only about half that in Stein's MCM-41-based mesostructure (Table 2), the greater pore diameter of the former affords complete access of mercury ions to its

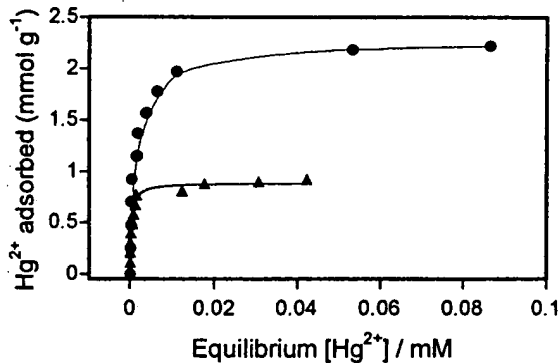


Fig. 4. Hg<sup>2+</sup> adsorption isotherms for MP(1)-MSU-2 (▲) and MP(2)-MSU-2 (●).

**Table 2**

Comparison between the physicochemical properties and mercury ion adsorption properties of reported thiol-functionalized mesostructures

Adsorbent	Synthesis method	Pore diameter (nm)	Thiol content (mmol/g)	Hg <sup>2+</sup> adsorption capacity (mmol/g)	Hg/S molar ratio
FMMS [6]	Grafting	4.0	3.2	2.5	0.78
MP(2)-MSU-2 (this work)	One-step	2.8	2.3	2.3	1.0
MP-MCM-41 (Stein) [8]	One-step	1.4	4.7	2.1	0.45
MP-HMS-C12 [5,9]	Grafting	2.7	1.5	1.5	1.0
MP-MSU-2 (this work)	One-step	4.2	0.9	0.90	1
MP-PCH [7]	Grafting	<1.0	1.1	0.74	0.67
MP-MCM-41 (Mercier) [9]	Grafting	2.0	0.57	0.59	1.0
MP-HMS-C8 [9]	Grafting	1.5	0.90	0.55	0.61

binding sites. As a result, the Hg<sup>2+</sup> adsorption capacity of MP(2)-MSU-2 slightly supercedes that of the functionalized MCM-41 material. Furthermore, the diffusion of the mercury ions into the MP(2)-MSU-2 pore channels is likely to be more favored owing to its significantly larger pore size.

Remarkably, no significant uptake of the other metals by the adsorbent was observed under the experimental conditions used, even at low metal concentrations where competition for the binding sites is not expected to occur. These observations, consistent with recently reported results [10], indicate that the thiol-functionalized mesostructures exhibit an unusual lack of affinity towards metals such as Pb<sup>2+</sup>, Cd<sup>2+</sup> and Zn<sup>2+</sup>, which normally bind efficiently to surface-anchored thiol moieties at neutral pH [1,2]. This demonstrates the usefulness of these materials as a highly mercury-selective adsorbent, capable of removing trace levels of Hg<sup>2+</sup> from a solution containing a variety of other ions which would normally compete for the occupancy of the binding sites in other metal ion adsorbents.

### 3.3. Adsorbent regeneration

Treatment of the mercury-loaded material with concentrated HCl (12.1 M) resulted in the complete removal of the bound Hg<sup>2+</sup> from the structure, regenerating the adsorbent for further metal ion uptake. The mercury ion uptake capacity of the regenerated material, however, dropped to 1.3 mmol/g, or to about 60% of its original adsorp-

tion capacity. A similar reduction of performance was also reported for acid-regenerated FMMS [6], suggesting that the acid-leaching method is at least partially destructive towards the mesostructures. These results suggest that, despite the effectiveness of the acid regeneration technique, other more benign regeneration techniques should be explored.

### 4. Conclusions

This work has demonstrated a practical new synthesis strategy for the preparation of mesoporous mercury ion adsorbents. One material prepared by the new technique had a pore structure, composition and Hg loading capacity comparable to that of FMMS (the highest capacity mesostructured mercury adsorbent known to date) [6], but whose synthesis has been greatly simplified. For the first time, a one-step synthesis procedure was used to yield a highly thiol-functionalized mesostructure which retained channels with mesopore-range dimensions (diameters > 2.0 nm). The synthesis method presented in this paper may also prove to be more cost-effective than that used to prepare FMMS because it allows the recovery of the expensive assembly surfactant, requires fewer preparative steps and reagents, and is accomplished in a much shorter time span. Because of its ability to increase the pore size by temperature control, the non-ionic surfactant assembly technique used has also been found to be a versatile alternative to the more conventional electrostatic templating method for the one-step preparation of

highly functionalized hybrid organic–inorganic mesostructures, extending the mesostructure channel diameters well beyond the micropore size range.

### Acknowledgements

The authors would like to thank the Ontario Geosciences Centre (Sudbury, Ontario), Dr. Allan Palmer (Natural Resources Canada, Nepean, Ontario) and Dr. Glenn Facey (University of Ottawa NMR Laboratory) for providing instrumental services. We also gratefully acknowledge the Natural Sciences and Engineering Research Council of Canada (NSERC) and the Laurentian University Research Fund (LURF) for financial support.

### References

- [1] M. Volkan, D.Y. Ataman, A.G. Howard, *Analyst* 112 (1987) 1409.
- [2] L. Mercier, C. Detellier, *Environ. Sci. Technol.* 29 (1995) 1318.
- [3] R.M. Izatt, J.S. Bradshaw, R.L. Bruening, *Pure Appl. Chem.* 68 (1996) 1237.
- [4] A.E. Gash, A.L. Spain, L.M. Dysleski, C.J. Flaschenriem, A. Kalaveshi, P.K. Dorhout, S.H. Strauss, *Environ. Sci. Technol.* 32 (1998) 1007.
- [5] L. Mercier, T.J. Pinnavaia, *Adv. Mater.* 9 (1997) 500.
- [6] X. Feng, G.E. Fryxell, L.-Q. Wang, A.Y. Kim, J. Liu, K.M. Kemner, *Science* 276 (1997) 923.
- [7] L. Mercier, T.J. Pinnavaia, *Micropor. Mesopor. Mater.* 20 (1998) 101.
- [8] M.H. Lim, C.F. Blanford, A. Stein, *Chem. Mater.* 10 (1998) 467.
- [9] L. Mercier, T.J. Pinnavaia, *Environ. Sci. Technol.* 32 (1998) 2749.
- [10] J. Brown, L. Mercier, T.J. Pinnavaia, *J. Chem. Soc., Chem. Commun.* (1999) 69.
- [11] S.L. Burkett, S.D. Sims, S.J. Mann, *J. Chem. Soc., Chem. Commun.* (1996) 1367.
- [12] C.E. Fowler, S.L. Burkett, S.J. Mann, *J. Chem. Soc., Chem. Commun.* (1997) 1769.
- [13] S.A. Bagshaw, E. Prouzet, T.J. Pinnavaia, *Science* 269 (1995) 1242.
- [14] E. Prouzet, T.J. Pinnavaia, *Angew. Chem., Int. Ed. Engl.* 36 (1997) 516.
- [15] R. Richer, L. Mercier, *J. Chem. Soc., Chem. Commun.* (1998) 1775.
- [16] G. Horvath, K.J. Kawazoe, *J. Chem. Eng. Jpn.* 16 (1983) 470.